XL CILAMCE
IBERO-LATIN AMERICAN CONGRESS ON COMPUTATIONAL METHODS IN ENGINEERING
NOVEMBER 11-14, 2019
Praiamar Natal Hotel & Convention Natal, RN-BRAZIL

COMPUTATIONAL SIMULATION AND ANALYTICAL PREDICTION OF AMMONIA LEAKAGE FOR HAZARDOUS AREA CLASSIFICATION

Claudemi A. Nascimento
Francisco J. Queiroz
Paloma L. Barros
Ranny R. Freire
Antônio T. P. Neto
José J. N. Alves
claudemi.alves@eq.ufcg.edu.br
josimar.queiroz@eq.ufcg.edu.br
paloma.lins@eq.ufcg.edu.br
ranny.freire@eq.ufcg.edu.br
tavernard@eq.ufcg.edu.br
jailson@eq.ufcg.edu.br
Federal University of Campina Grande
882 Aprígio Veloso Av., 58429-900, Paraíba, Brazil

Abstract. Ammonia is widely used in several chemical and food industries around the world, nevertheless it is a toxic and flammable component which may cause accidents due to leakage and dispersion. The international standard IEC 60079-10-1 regards flammable components leakage, it accounts criteria and guidelines for explosive atmosphere formation and reducing the risk of explosion. The standard claims, based on experiences, that a release of ammonia vapor will often dissipate rapidly in the open air. This scenario will result in a negligible hazardous area extent in most cases. Hence, this work aims to investigate ammonia leakage in open air under different leakage conditions. For this purpose, the authors compared the extent of hazardous area, at the Lower Flammable Limit (LFL), using analytical models with those obtained from a 2D Computational Fluid Dynamics model. The CFD model was able to predict a characteristic barrel pattern at the exit of the leaking orifice, typical of choked flow. The results obtained from analytical models show that the extent of hazardous area was overestimated compared to the CFD model. Among the analytical models used in this study, Souza's, Tommasini's, and Ewan and Moodie's yielded results were closer to the CFD model. Furthermore, the extent of hazardous area for ammonia release are small, just as the plume volume, when compared to definitions presented at the international standard IEC 60079-10-1.

Keywords: Ammonia leakage; Emission; CFD; Hazardous area

1 Introduction

Ammonia is used in a wide range of applications, including production of fertilizers and chemical products (based on ammonia). In addition, due to its physical and chemical properties this compound is also used as coolant gas in food preservation processes [1]. Studies regarding its dispersion are very important as a result of ammonia's broad applicability and high toxicity [2]. The higher the amount of ammonia used in industry, the higher is the number of ammonia leakage incidents [3].

The compound is stored in liquid state by applying pressure, its vapor pressure is equal to 8.852 bar at 21 °C, resulting in a high volatile substance. Several factors, such as sealing failures, corrosion and operational errors, can lead to leakage incidents which are likely to result in environmental pollution. The emission of ammonia may cause eye irritation and shortness of breath in humans [4]. In addition, ammonia/air mixture is flammable when ammonia volume concentration ranges from 15.7% to 27.4% [5]. Its dispersion is influenced by different release location, temperature, wind speed and direction [3].

The International Standard IEC 60079-10-1 [6], regarding area classification for explosive gas atmospheres, claims that, according to experience, an ammonia release rapidly dissipates outdoors. Then, the hazardous classified area will in most cases be negligible. This standard recommends the application of computational fluid dynamics (CFD) techniques to predict more reliable results in complex scenarios, which are likely to result in less costly area classification projects as long as the classified area probably wouldn't be overestimated.

Therefore, this work aims to investigate the behavior of an outdoor ammonia leak under different release conditions by using analytical models presented in the literature, and CFD, in order to evaluate the standard's claim.

2 Mathematical modeling

2.1 Gas dispersion modeling

Flammable gas is released through an orifice, it comes from the reservoir and disperses into the atmosphere, as shown in Fig. 1. Where T, P and ρ represent temperature, pressure, and density, respectively. The subscript characters 0, e, a represent, respectively, the following locations: reservoir, orifice and external ambient.

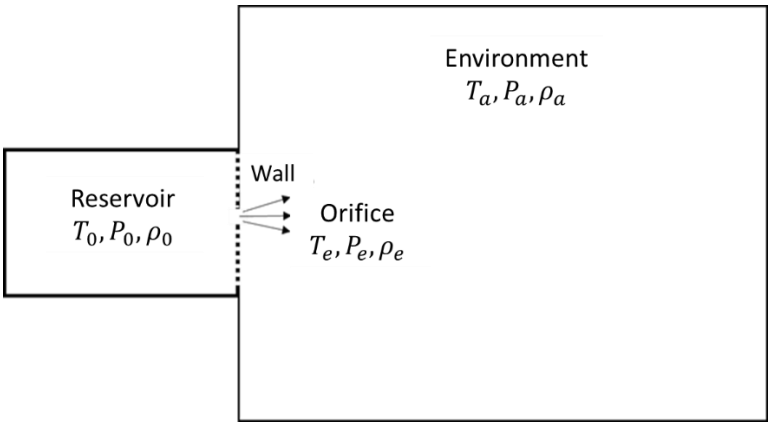

Figure 1. Gas release into the environment through the orifice

Mass and energy balances for isentropic flow can be used to estimate gas release rates. Table 1 presents the relations to calculate leakage conditions (under stagnation and external

ambient conditions) for subsonic and sonic cases [7]. Both stagnation temperature (T_0) and stagnation pressure (P_0) remain constant throughout the process.

Table 1. Leakage conditions as a function of ambient and stagnation conditions

Regime flow	Subsonic	Sonic
Condition	$\frac{P_a}{P_0} > \left(\frac{2}{\gamma+1}\right)^{\frac{\gamma}{\gamma-1}}$	$\frac{P_a}{P_0} \leq \left(\frac{2}{\gamma+1}\right)^{\frac{\gamma}{\gamma-1}}$
Temperature	$T_e = T_0\left(\frac{P_a}{P_0}\right)^{\frac{(\gamma-1)}{\gamma}}$	$T_e = T_0\left(\frac{2}{\gamma+1}\right)$
Pressure	$P_e = P_a$	$P_e = P_0\left(\frac{2}{\gamma+1}\right)^{\frac{\gamma}{\gamma-1}}$
Density	$\rho_e = \rho_0\left(\frac{P_a}{P_0}\right)^{\frac{1}{\gamma}}$	$\rho_e = \rho_0\left(\frac{2}{\gamma+1}\right)^{\frac{1}{\gamma-1}}$
Velocity	$v_e = \left(\frac{2\gamma}{\gamma-1}\frac{R}{P_0.W}T_0\left(1-\left(\frac{P_a}{P_0}\right)^{\frac{\gamma-1}{\gamma}}\right)\right)^{\frac{1}{2}}$	$v_e = \left(\frac{2\gamma}{\gamma+1}\frac{R}{W}\,T_0\right)^{\frac{1}{2}}$
Mass flow	$m_e = A_e\left(\frac{2\gamma}{\gamma-1}\frac{P_0W}{RT_0}T_0\left(1-\left(\frac{P_a}{P_0}\right)^{\frac{\gamma-1}{\gamma}}\right)\right)^{\frac{1}{2}}$	$m_e = A_eP_0\left(\frac{W\gamma}{RT_0}\left(\frac{2}{\gamma+1}\right)^{\frac{\gamma+1}{\gamma-1}}\right)^{\frac{1}{2}}$

Where $\gamma=C_p/C_v$ is the Poisson's ratio, C_v is the specific heat at constant volume, ρ_0 is the specific mass under stagnation conditions, A_e is the orifice's cross sectional area, W is the gas molar mass, R is the universal gas constant, v_e is the exit velocity at the orifice exit, and m_e is the mass flow at the orifice exit.

2.2 Dispersion models

There are some analytical gas dispersion models to calculate the extent of hazardous areas available in the literature. The variable x_h' represents the axial length in which a gas/air mixture forms a flammable atmosphere. In addition to the extent of the hazardous area, some models (by inserting a Gaussian radial dispersion term) are able to predict the volume of the flammable plume formed (V_c) [8].

These analytical models result from mass balance and momentum equations combined with parameters found by experiments. The models take into account the following factors: flow regime, gas physical properties (density, molar mass and flammability limits), orifice diameter,

and physical properties of the external ambient and release source, such as pressure and temperature [8].

A summary of the models used for both extent of the hazardous area and flammable plume volume determination is given by Table 2. Further details on these models can be found in Lees [8] e Alves *et al*. [9].

Table 2. Summary of analytical models used to determine hazardous extent and flammable feather volume

Reference	Extent to LFL	Flammable plume volume
Italian Classification Guide CEI 31-35 [10] (m)]	$x'_h = 5.2\sqrt{P_0.A_e}\frac{K_z}{E}W^{-0.4}; K_z = 1$	-
McMillan's sonic model [11] (m)	$x'_h = 2.1\cdot 10^3\left[\frac{m_e}{(E)^2.W^{1.5}.T_0^{0.5}}\right]$	-
Long's subsonic model [8] (m)	$x'_h = k_2\left(\frac{d_e}{Y_m^{LFL}}\right)\cdot\left(\frac{\rho_e}{\rho_{ga}}\right)^{\frac{1}{2}} - x_{v3}$ $k_2 = 6; k_3 = 5;\ x_{v3} = k_2 d_e\left(\frac{\rho_e}{\rho_{ga}}\right)^{\frac{1}{2}}$	$Vc = \frac{\pi.{x'_h}^3}{3k_3}\left[\frac{1}{3} - \ln\left(\frac{Y_m^{LFL}.x'_h}{k_2.d_e.\left(\frac{\rho_e}{\rho_{ga}}\right)^{\frac{1}{2}}}\right)\right]$
Ewan and Moodie's sonic model [12] (m)	$x'_h = \frac{x_c.\ln(1-Y_m^{LFL})-1}{\ln(1-Y_m^{LFL})\cdot\left(\frac{k'}{r_{eq}}\right)\cdot\left(\frac{\rho_{ga}}{\rho_{eq}}\right)^{\frac{1}{2}}}$ $k' = 0.104; x_c = 0.7; b_2 = 23 + 41\cdot\rho'_{ga}$	$V_c = \frac{\pi.{x'_h}^3}{3b_2}\left[\frac{1}{3} - \ln\left(\frac{k'.Y_m^{LFL}.x'_h}{r_{eq}.\left(\frac{\rho_{eq}}{\rho_{ga}}\right)^{\frac{1}{2}}}\right)\right]$
Yellow book sonic model [8] (m)	$x'_h = \frac{\left(\frac{b_1+b_2}{b1}\right)-(1-\rho'_{ga})Y_m^{LFL}}{k_1\left(\frac{Y_m^{LFL}}{d_{eq}}\right)\cdot\left(\frac{\rho'_{ga}}{(\rho'_{eq})^{\frac{1}{2}}}\right)} - x_{v4}$ $k_1 = 0.32;\ b_1 = 50.5 + 48.2\cdot\rho'_{ga} - 9.95\cdot{\rho'_{ga}}^2;\ x_{v4} = \frac{\left(\left(\frac{b1+b2}{b1}\right).(\rho'_{eq}) - 1 + \rho'_{ga}\right)}{\left(\frac{k_1}{d_{eq}}\right)\left(\frac{\rho'_{ga}}{(\rho'_{eq})^{\frac{1}{2}}}\right)};$	$V_c = \frac{\pi.{x'_h}^3}{3b_2}\left[\frac{1}{3} - \ln\left(\frac{k_1.b_1.\left(\frac{\rho'_{ga}}{(\rho'_{eq})^{\frac{1}{2}}}\right)Y_m^{LFL}.x'_h}{d_{eq}.\rho'_{eq}.(b1+b2)}\right)\right]$
Souza's model [13] (m)	$x'_h = 0.11\frac{d_e}{E}\sqrt{\frac{P_0}{\sqrt{T_0.W}}}$	-

Where:

b_1,b_2 are Yellow Book model's empirical parameters [-];
d_e is the orifice's diameter [m];
d_{eq} is the equivalent diameter of the gas source [m];
E is the gas lower flammability limit [% volume]
k' is a constant in Ewan and Moodie's model [-];
k_1 is a constant in Yellow book model [-];
k_2, k_3 are Long model's constants [-];
K_z is a parameter to take into account the background concentration [-];

r_{eq} is the orifice's radius [-]
x_c is a Ewan and Mopdie model's constant [-];
Y_m^{LFL} is the gas mass fraction to the lower flammability limit [-];
ρ_e is the gas density at exit conditions [kg/m^3];
$\rho_e{}'$ is the normalized density of the gas at exit conditions (normalized to air's density) [-];
ρ_{eq} is the density of the gas at the equivalent diameter at exit conditions [kg/m^3];
ρ'_{eq} is the normalized density of the gas at the equivalent diameter at exit conditions (normalized to air's density) [-];
ρ_{ga} is the density of the gas at atmospheric conditions [kg/m^3];
ρ'_{ga} is the normalized density of the gas at atmospheric conditions (normalized to air's density) [-].

2.3 CFD modeling

CFD modeling is based on global mass conservation, momentum and energy hydrodynamic equations as follows [14]:

$$\frac{\partial \rho}{\partial t} + \nabla \cdot (\rho \boldsymbol{U}) = 0 \tag{1}$$

$$\frac{\partial (\rho Y_i)}{\partial t} + \nabla \cdot (\rho \boldsymbol{U} Y_i) = \nabla \cdot (\Gamma_{\mathrm{iM}} \nabla Y_i) \tag{2}$$

$$\frac{\partial (\rho \boldsymbol{U})}{\partial t} + \nabla \cdot (\rho \boldsymbol{U} \otimes \boldsymbol{U}) = -\nabla \mathrm{p} + \nabla \cdot \tau \tag{3}$$

$$\frac{\partial (\rho h)}{\partial t} + \nabla \cdot (\rho \boldsymbol{U} h) = \nabla \cdot (\lambda \nabla \mathrm{T}) + \tau : \nabla \mathbf{U} \tag{4}$$

Where ρ is the mixture density, $\boldsymbol{U}$ is the vector velocity, Y_i is the mass fraction of component i, $\Gamma_{\mathrm{iM}}$is the effective mass diffusivity of the component i in the mixture, p is the pressure, τ is the stress tensor, h is the enthalpy, λ is the effective thermal conductivity, T is the temperature, and t is the time.

3 Methodology

3.1 Geometry and mesh

For ammonia leakage simulation, the adopted geometry consists of a 4-degree slice of a 3-tridimensional computational domain, which can be considered as a 2-dimensional model due to symmetry conditions. The geometry is made up by a reservoir (which corresponds to the vessel), an orifice, and the external ambient. The out-of-scale geometry and its dimensions are detailed in Fig. 2 and 3, respectively.

Considering the boundary conditions for the four separated regions depicted in Figure 2, which will be defined at a later stage, the geometry contours are assigned for each one as follows: (1) Reservoir conditions (pressure and temperature); (2) Wall with non-slip condition; (3) Opening condition (allowing input and output flows within the domain, considering external ambient temperature and pressure); (4) Axisymmetric condition, buoyancy was neglected.

A mesh dependency study was performed, and a structured hexahedral numerical mesh containing 163,151 elements and 23,125 nodes was adopted. Due to high pressure gradients near the orifice, more refinement is demanded around it. Higher refinement levels ensure that the shockwave phenomenon is better predicted by the simulation. However, as the distance to the orifice increases, lesser refinement is necessary due to the low gradients. More details about mesh construction can be found in Souza *et al*. [15]

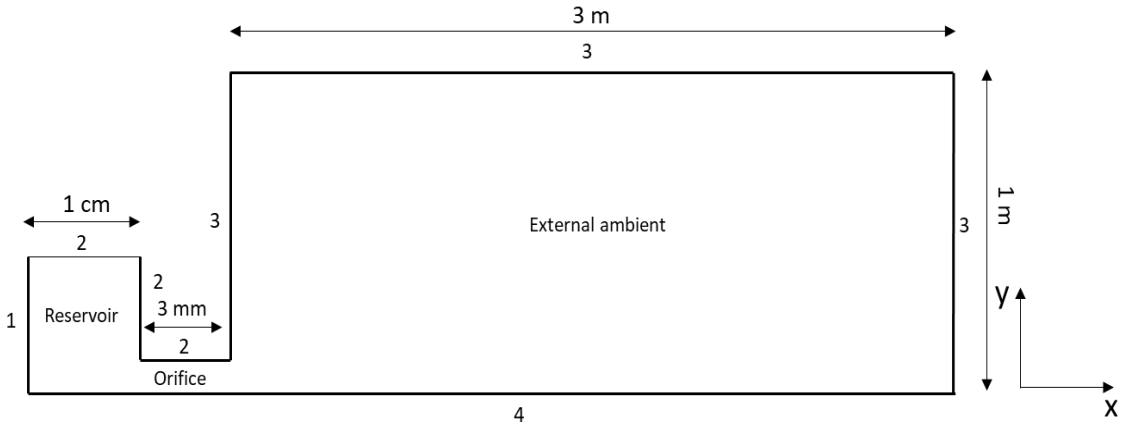

Figure 2. Geometry configuration and its dimensions.

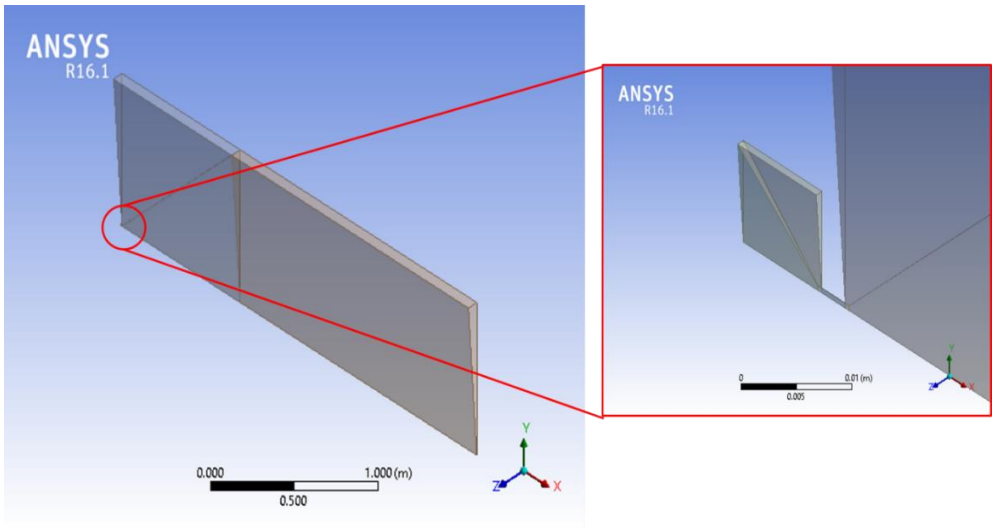

Figure 3. Computational domain applied in the simulation.

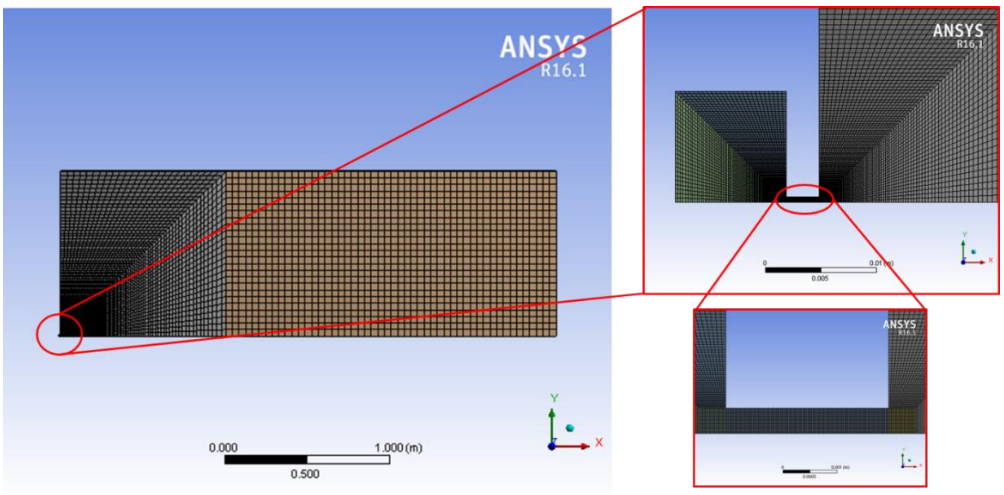

Figure 4. Computational numerical mesh.

3.2 Numerical simulation

The numerical simulation was performed in ANSYS CFX 16.1® software. The release consists of ammonia vapor stored in the reservoir under two different stagnation pressures (4 bar and 10 bar) at the temperature of 30 °C. In addition to different storage conditions, in order to analyze the influence of different orifice sizes, simulations with five different diameters ranging from 0.1 mm to 2.5 mm were performed. Table 3 shows a summary of the model specifications.

Regarding its nature, the flow is non-isothermal, compressible and turbulent under steady state condition. In this work a Shear Stress Transport (SST) turbulence model was used, as recommended by Papanikolaou *et al*. [16]. This turbulence model combines k-ϵ model (for regions far from walls) and k-ω (for regions near walls, which provides better results than k-ϵ model in such case).

Table 3. Simulated gas and geometry specifications

Gas	Storage pressure (bar)		Storage Temperature (°C)	Orifice diameters (mm)
Amônia	4	10	30	0.1 0.25 1 1.25 2.5

4 Results and discussion

4.1 Model validation

The CFD model, capable of predicting the flow nature, was validated. It is known by the formation of a barrel soon after the gas release through the orifice, which can be calculated by analytical expressions. The barrel length for a storage pressure of 10 bar, obtained by CFD model (Fig.5) was compared to Ashkenas and Sherman's model, calculated by Eq. (5). In Table 4, it is possible to verify that the results obtained by the CFD model agrees with Ashkenas and Sherman's [17]. Similar comparisons of barrel length were performed by Alves *et al.* [9] using different leakage conditions.

$$Barrel's\ length = 0.67 d_e \left(\frac{P_0}{P_a}\right)^{0.5} \tag{5}$$

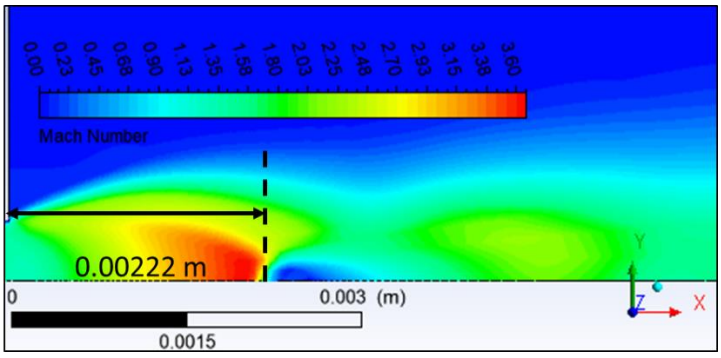

Figure 5. CFD barrel length considering a storage pressure and temperature of 10 bar and 30 ° C respectively.

Table 4. Barrel lengths comparison

Storage pressure (bar)	Barrel length (m)	
	Ashkenas and Sherman [17]	CFD
10	0.00212	0.00222

4.2 CFD model validation based on analytical models

According to analytical models, the hazardous area extent to LFL, for different orifice's diameters and pressures, were compared with those obtained from the CFD model. Table 5 presents the results.

The analyzes of the results provided by CFD and analytical models shows that sonic models fit best the CFD results, such as those proposed by Ewan and Moodie. [12], Tommasini [10] and Souza *et al*. [13], as shown in Table 6. The results show that this more adequate adjustment is due to better parameter estimation method and specific assumptions related to simulation release conditions. Conversely, the results achieved for subsonic Long model [8] are quite unsatisfactory, proving that is not suitable for such situation.

Table 5. Summary of analytical models used to determine hazardous area extent and flammable plume volume

Diameter (mm)	Italian Classification Guide CEI 31-35 [10] (m)	McMillan's sonic model [11] (m)	Long's subsonic model [8] (m)	Ewan and Moodie's sonic model [12] (m)	Yellow book sonic model [8] (m)	Souza's model [13] (m)	CFD (m)
Ammonia at 4 bar and 30 °C							
0.10	0.006	0.009	0.007	0.006	0.007	0.005	0.005
0.25	0.016	0.023	0.017	0.015	0.017	0.014	0.012
1.00	0.063	0.093	0.070	0.058	0.068	0.055	0.049
1.25	0.079	0.116	0.087	0.072	0.085	0.068	0.064
2.50	0.157	0.232	0.174	0.144	0.170	0.137	0.122
Ammonia at 10 bar and 30°C							
0.10	0.010	0.015	0.011	0.009	0.011	0.009	0.007
0.25	0.025	0.037	0.028	0.023	0.027	0.022	0.018
1.00	0.099	0.147	0.110	0.091	0.107	0.087	0.073
1.25	0.124	0.184	0.138	0.114	0.134	0.108	0.093
2.50	0.247	0.367	0.276	0.228	0.268	0.216	0.184

Table 6. Average difference of analytical relative to CFD results.

	Italian Classification Guide CEI 31-35 [10] (m)	McMillan's sonic model [11] (m)	Long's subsonic model [8] (m)	Ewan and Moodie's sonic model [12] (m)	Yellow book sonic model [8] (m)	Souza's model [13] (m)
Average relative difference (%)	30.41	48.18	45.04	20.29	41.52	13.86

4.3 CFD model results compared to IEC 60079-10-1 standard

The standard claims, based on experience, that a release of ammonia vapor will often dissipate rapidly into the open air. This scenario will result in a negligible hazardous area extent in most cases. With the purpose of evaluating this claim, the flammable plume volume at LFL was calculated by using analytical models (shown in Table 2). The comparison of the analytical models results to CFD model is presented in Table 7.

For flammable plume volumes up to 0.1m^3, the standard IEC 60079-10-1 [6] classifies the environment dilution as high. In these cases, unless for a poor ventilation availability condition, there will be a zone of negligible hazardous area extent (for both fair and good ventilation availability conditions). In case of poor ventilation availability, the area will be classified as a zone 2, and its extent will be negligible or not. However, in this case, given the impossibility of assessing the hazardous area extent to LFL from the standard charts (due to low characteristic release values shown in Table 8), negligible hazardous area extents were also be considered. The results in Table 8 represents the volumetric flow rate in which the LFL is reached and those were calculated by Eq. (6).

Therefore, the results obtained from the CFD model for flammable plume volumes, endorsed by the analytical models, allowed to conclude that such volumes are in fact smaller than 0.1 m^3. Thus, a flammable gas atmosphere formed from the release of ammonia, treated as a jet release, can be considered as being of negligible extent as suggests the standard.

$$Release\ characteristic = \frac{m_e}{\rho_e . k . LFL} \tag{6}$$

Where k is a safety factor between 0 and 1.

Table 7. Ammonia vapor flammable plume volume at different analytical and CFD models

Diameter (mm)	Long's subsonic model [8] (m^3)	Yellow book sonic model [8] (m^3)	Ewan and Moodie's sonic model [12] (m^3)	CFD (m^3)
Ammonia at 10 bar and 30 °C				
0.10	1.22E-07	1.19E-08	6.77E-09	1.65E-06
0.25	1.90E-06	1.85E-07	1.06E-07	2.46E-05
1.00	1.22E-04	1.19E-05	6.75E-06	1.66E-03
1.25	2.37E-04	2.32E-05	1.32E-05	3.32E-03
2.50	1.90E-03	1.85E-04	1.05E-04	2.60E-02

Table 8. Release characteristic according to IEC 60079-10-1 [6]

Diameter (mm)	Release characteristic (m^3/s)
Ammonia at 10 bar and 30 °C	
0.10	1.330E-06
0.25	8.316E-06
1.00	1.330E-04
1.25	2.079E-04
2.50	8.316E-04

5 Final considerations

The validation of the proposed CFD model was performed from the barrel length analysis, and the result compared to the analytical model proposed by Ashkenas and Sherman [17] proved to be satisfactory.

After validating the CFD model from the barrel length analysis by the analytical model Ashkenas and Sherman [17], the results were compared those obtained by the analytical models for hazardous area extent shown in Table 2. The evaluations enable to conclude that the models proposed by Ewan and Moodie [12], Tommasini [10] and Souza *et al*. [13] presented flammable atmosphere extension values close to the results obtained in CFD. Nonetheless, when it comes to other models, the results were inaccurate, probably due to the different conditions and specific assumptions used to obtain the analytical models.

Using the analytical and CFD models, the flammable plume volume values formed from ammonia release at LFL were evaluated. Based on the results and international standard's recommendations [6], it can be concluded that the calculated flammable plume volumes much smaller than 0.1 m^3 are zones in which its extent are probably negligible. It ensures that the standard's claim that an ammonia release rapidly dissipates into the environment, thus a flammable gas atmosphere will in most cases be negligible.

Acknowledgements

The authors thank Capes **f**or financial support for this study.

References

[1] C. Cheng, W. Tan and L. Liu. Numerical simulation of water curtain application for ammonia release dispersion. *J. Loss Prev. Process Industries*, vol. 30, pp. 105-112, 2014.

[2] R. Bouet, S. Duplantier and O. Salvi. Ammonia large scale atmospheric dispersion experiments in industrial configurations. *J. Loss Prev. Process Industries*, vol. 18, pp. 512-519, 2005.

[3] W. Tan, H. Du, L. Liu, T. Su and X. Liu. Experimental and numerical study of ammonia leakage and dispersion in a food factory. *J. Loss Prev. Process Industries*, vol. 47, pp. 129-139, 2017.

[4] R. K. Gangopadhyay and S. K. Das. Ammonia leakage from refrigeration plant and the management practice. *Process Saf. Pro.*, vol. 27, pp. 15-20, 2010.

[5] R. F. Griffiths and L.C. Megson. The effect of uncertainties in human toxic response on hazard range estimation for ammonia and chlorine. *Atmos. Environ*., vol. 18, pp. 1195-1206, 1984.

[6] IEC 60079-10-1/Ed2. Explosive Atmospheres – Part 10-1: Classification of Areas – Explosive Gas Atmospheres, 2015.

[7] L.E. Sissom and D. R. Pitts. *Elements of Transport Phenomena*. McGraw-Hill BookCompany, New York, USA, 1972.

[8] F.P. Lees. *Loss Prevention in the Process Industries: Hazard Identification*, Vol.1., 2Rev ed. Assessment and Control, 1996.

[9] J. J. N. Alves, A. T. P. Neto, A. C. B. Araujo, H. B. Silva, S. K. Silva, C. A. Nascimento, and A. M. Luiz. Overview and experimental verification of models to classify hazardous areas. Process Safety and Environmental Protection, v. 122, pp. 102-117, 2019.

[10] R. Tommasini. The classification of hazardous areas where explosive gas atmospheres may be present. *Saf. Sci*., vol. 58, pp. 53–58, 2013.

[11] A. McMillan. *Electrical installations in hazardous area*. Elsevier Science LTD, 1998.

[12] B.C.R. Ewan and K. Moodie. Structure and velocity measurements in under-expanded jets. *Combust. Sci. Technol*., vol. 45, pp. 275–288, 1986.

[13] A. O. Souza, A. M. Luiz, A. T. P. Neto, A. C. B. Araujo, H. B. Silva, K. S. Silva, and J. J. N. Alves. A new correlation for hazardous area classification based on experiments and CFD predictions. *Process Safety Progress*, v. 38, n. 1, pp. 21-26, 2018a.

[14] ANSYS, 2015. Ansys CFX-Solver Theory Guide. Ansys Inc., Canonsburg, USA.
[15] A. O. Souza, A. M. Luiz, A. T. P. Neto, A. C. B. Araujo, H. B. Silva, K. S. Silva, and J. J. N. Alves. CFD predictions for hazardous area classification. *Chin. J. Chem. Eng.*, vol. 27, pp. 21-31, 2018b.
[16] E. Papanikolaou, D. Baraldi, M. Kuznetsov and A. Venetsanos. Evaluation ofnotional nozzle approaches for CFD simulations of free-shear under-expanded hydrogens jets. *Int. J. Hydrogen Energy*, vol. 37, pp. 18563–18574, 2012.
[17] H. Ashkenas and F.S. Sherman. *Rarefied gas dynamics*. J.H. de Leeuw (Ed.), *AIAAJ*., vol. 30, pp. 1657-1659, 1966.